Photochemical processes involving the UV absorber benzophenone-4 (2-hydroxy-4-methoxybenzophenone-5-sulphonic acid) in

(Article begins on next page)

23 April 2024

Photochemical processes involving the UV absorber benzophenone-4 (2-hydroxy-4-methoxybenzophenone-5-sulphonic acid) in aqueous solution. Reaction pathways and implications for surface waters.

Elisa De Laurentiis,[a] Marco Minella,[a] Mohamed Sarakha,[b,c] Alessandro Marrese,[a] Claudio Minero,[a] Gilles Mailhot,[b,c] Marcello Brigante [b,c]* and Davide Vione [a,d]*

[a] *Università degli Studi di Torino, Dipartimento di Chimica, Via P. Giuria 5, 10125 Torino, Italy. http://www.chimicadellambiente.unito.it*

[b] *Clermont Université, Université Blaise Pascal, Institut de Chimie de Clermont-Ferrand, BP 10448, F-63000 Clermont-Ferrand, France.*

[c] *CNRS, UMR 6296, ICCF, BP 80026, F-63177 Aubière, France.*

[d] *Università degli Studi di Torino, Centro Interdipartimentale NatRisk, Via L. Da Vinci 44, 10095 Grugliasco (TO), Italy. http://www.natrisk.org*

* Address correspondence to either author. E-mail: davide.vione@unito.it; marcello.brigante@univ-bpclermont.fr

Abstract

The sunlight filter benzophenone-4 (BP-4) is present in surface waters as two prevailing forms, the singly deprotonated (HA$^-$) and the doubly deprotonated one (A^{2-}), with pK$_{a2}$ = 7.30±0.14 (μ±σ, by dissociation of the phenolic group). In freshwater environments, BP-4 would mainly undergo degradation by reaction with $^\bullet$OH and direct photolysis. The form HA$^-$ has a second-order reaction rate constant with $^\bullet$OH ($k_{\bullet_{OH}}$) of (1.87±0.31)·10^{10} M^{-1} s^{-1} and direct photolysis quantum yield Φ equal to (3.2±0.6)·10^{-5}. The form A^{2-} has (8.46±0.24)·10^9 M^{-1} s^{-1} as the reaction rate constant with $^\bullet$OH and (7.0±1.3)·10^{-5} as the photolysis quantum yield. The direct photolysis of HA$^-$ likely proceeds *via* homolytic breaking of the O-H bond of the phenolic group to give the corresponding phenoxy radical, as suggested by laser flash photolysis experiments. Photochemical modelling shows that because of more efficient direct photolysis (due to both higher sunlight absorption and higher photolysis quantum yield), the A^{2-} form can be degraded up to 3 times faster than HA$^-$ in surface waters. An exception is represented by low-DOC (dissolved organic carbon) conditions, where the $^\bullet$OH reaction dominates degradation and the transformation kinetics of HA$^-$ is faster compared to A^{2-}. The half-life time of BP-4 in mid-latitude summertime would be in the range of days to weeks, depending on the environmental conditions. BP-4 also reacts with Br$_2$$^{-\bullet}$, and a rate constant $k_{Br_2^{-\bullet},BP-4}$ = (8.05±1.33)·10^8 M^{-1} s^{-1} was measured at pH 7.5. Model results show that reaction with Br$_2$$^{-\bullet}$ could be a potentially important transformation pathway of BP-4 in bromide-rich (*e.g.* seawater) and DOM-rich environments.

1. *Introduction*

Due to its ability to significantly absorb UVA and UVB radiation without undergoing fast transformation, the UV filter BP-4 (2-hydroxy-4-methoxybenzophenone-5-sulphonic acid) is extensively used in sunscreen formulations and as an anti-UV agent in many products such as cosmetics, plastics, packages and films (Díaz-Cruz and Barceló, 2009; De Coster and van Larebeke, 2012). As a consequence of its widespread use in both recreational and technological contexts, of its chemical stability and resistance to biodegradation, BP-4 is being increasingly detected in surface waters (Poiger et al. 2004). It can reach surface waters directly from skin washing and from incomplete degradation in wastewater treatment plants (WWTPs) (Fent et al., 2010). BP-4 undergoes some degradation in WWTPs, but incomplete removal combined with elevated concentration values in the influent causes significant emission by WWTPs into surface waters (Wick et al., 2010). Incomplete removal of BP-4 in WWTPs suggests that this compound might undergo limited biodegradation in water bodies.

The BP-4 levels that are commonly found in surface waters (in the low µg L^{-1} range; Fent et al., 2010) are generally too low to cause acute toxicity (Fent et al., 2010a), but chronic effects cannot be excluded. Indeed, *in vitro* tests have shown that BP-4 has anti-estrogenic and anti-androgenic activity (Kunz and Fent, 2006), but also estrogenic activity in fish (Inui et al., 2003; Kunz et al., 2006). As far as human exposure is concerned, the only available data are related to allergic reactions upon dermal contact with products containing BP-4 (Alanko et al., 2001; Caruana et al., 2011). However, concentrations involved are much higher than those found in environmental waters.

Organic compounds that occur in aqueous environments can be transformed by a variety of abiotic and biological pathways, among which direct photochemistry and photogenerated reactive species such as hydroxyl radical ($^{\bullet}$OH), carbonate radical ($CO_3^{\bullet-}$), singlet oxygen ($^1O_2$) and triplet states of Chromophoric Dissolved Organic Matter ($^3CDOM^*$) (Mack and Bolton, 1999; Canonica et al., 1995 and 2005; Canonica and Freiburghaus, 2001; Gerecke et al., 2001; Boreen et al., 2003; Page et al., 2011).

An important problem in the study of photochemical transformation processes of water-dissolved pollutants is the difficulty to satisfactorily simulate in the laboratory the extreme variability of environmental conditions. An alternative approach that overcomes this difficulty is the prediction of the photodegradation kinetics of organic xenobiotics in surface waters on the basis of water chemistry and depth and of photochemical reactivity parameters (direct photolysis quantum

yields and reaction rate constants with $^\bullet OH$, $CO_3^{\bullet-}$, $^1O_2$ and $^3CDOM^*$). We have recently developed a photochemical model that helps performing this task and that has been validated against the transformation of several organic pollutants in fresh and estuarine (brackish) water (Maddigapu et al., 2011; Vione et al., 2011a; De Laurentiis et al., 2012a; Sur et al., 2012). In this context, the purpose of the present paper is to predict the photochemical transformation kinetics of BP-4 in natural water systems, to gain insight into its environmental persistence. To do so, we have measured direct photolysis quantum yields and second-order rate constants of potentially significant photoinduced processes, using them as input data for the photochemical model. A further issue is the direct emission of BP-4 into coastal seawater, which is enabled by its use in sunscreen formulations. The ion Br^- is the main $^\bullet OH$ scavenger in saltwater, thus we have studied the reactivity between BP-4 and the radical $Br_2^{\bullet-}$. The latter can be produced upon oxidation of bromide by $^\bullet OH$ and by $^3CDOM^*$, and the two processes are operational under different environmental conditions (De Laurentiis et al., 2012b). By coupling laboratory measures and modelling, it was possible to assess the impact of bromide on the transformation kinetics of BP-4. To our knowledge, few or no data are presently available about the phototransformation of BP-4 in surface waters, and the present paper is intended to help filling this knowledge gap.

2. Experimental

For the reagents' list see the Supplementary Material (hereafter SM).

2.1. Determination of pK_a

The pK_a value of the sulphonic group of BP-4 is reported in the literature (pK_{a1} = -0.70; Negreira et al., 2009). We could not find a reference for the acid-base equilibrium of the phenolic group (pK_{a2}), despite experimental evidence that such equilibrium would be important at the typical pH values of surface waters. For this reason, the pK_{a2} was spectrophotometrically determined (see the Supplementary Material, hereafter SM, for the procedure).

2.2. Irradiation experiments

The irradiation set-ups used for the screening study of BP-4 reactivity are described in SM, together with the relevant results.

After obtaining evidence that direct photolysis and reaction with $^\bullet OH$ would be the main transformation pathways of BP-4 in surface waters, the kinetics of these processes was studied at pH values where the anionic and dianionic BP4 forms would prevail (pH 4 and 10, respectively). Solutions to be irradiated (5 mL) were placed in cylindrical Pyrex glass cells (4.0 cm diameter, 2.5 cm height, with a lateral neck and screw cap), which were placed under the lamp and magnetically

stirred during irradiation. "Blank" experiments were carried out in the dark by wrapping the cells in double aluminium foil and by placing them under the same lamp used for irradiation. Direct photolysis and reaction with $^\bullet$OH were studied upon irradiation with a Philips TL 01 lamp, which produced 6.20 ± 0.35 W m^{-2} irradiance on top of the solutions. Irradiance was measured with a CO.FO.ME.GRA. (Milan, Italy) power meter. The photon flux in solution was $(4.1\pm0.3)\cdot10^{-6}$ Einstein L^{-1} s^{-1}, actinometrically determined with the ferrioxalate method. Because of the polychromatic emission spectrum of the lamp, we have taken into account: *(i)* the shape of the lamp spectrum (taken with a calibrated Ocean Optics USB 2000 CCD spectrophotometer though the same Pyrex window used in the irradiation cells); *(ii)* the absorption spectrum of the ferrioxalate solution and *(iii)* the quantum yield of Fe^{2+} generation upon ferrioxalate photolysis (Albinet et al., 2010). The emission spectrum of the lamp (spectral photon flux density, Einstein L^{-1} s^{-1} nm^{-1}, normalised to actinometry data) and the absorption spectra of the two relevant forms of BP-4 (molar absorption coefficients, L mol^{-1} cm^{-1}, measured with a Varian Cary 100 Scan UV-Vis spectrophotometer) are reported in Figure 1. The time trend of BP-4 upon irradiation was monitored by liquid chromatography with ion-coupling elution (see SM for details).

2.3. *Determination of reaction rates*

The time evolution data of BP-4 were fitted with pseudo-first order equations of the form $C_t = C_o\, e^{-kt}$, where C_t is the concentration of BP-4 at the time *t*, C_o its initial concentration and *k* (floating variable) the first-order rate constant of BP-4 transformation. The numerical fit was made on 5-6 data points per run, the irradiation time scale being 6 days for direct photolysis and 3 hours for the irradiation experiments in the presence of H$_2$O$_2$. Under the first-order approximation, the initial rate of BP-4 transformation is $R_o = k\,C_o$. The errors on the rates ($\pm\sigma$) were calculated taking into account the scattering of experimental data using the fit function.

2.4. *Laser flash photolysis measures*

Excitation experiments were carried out using the third harmonic (355 nm) of a Quanta Ray GCR 130-01 Nd:YAG laser system instrument, used in a right-angle geometry with respect to the monitoring light beam. The single pulses were *ca.* 9 ns in duration, with energy of ~ 90 mJ/pulse. The relative high laser energy was adopted in order to obtain a clear signal (absorbance of transient species) generated by the pulse and minimize the signal-to-noise ratio.

Moreover, the occurrence of monophotonic processes and the exclusion of biphotonic ones (possible at high pulse energy) was verified under the chosen conditions. The transient absorbance at the pre-selected wavelength was monitored by a detection system consisting of a pulsed xenon lamp (150 W), monochromator and a photomultiplier (1P28). A spectrometer control unit was used for synchronising the pulsed light source and programmable shutters with the laser output. The

signal from the photomultiplier was digitised by a programmable digital oscilloscope (HP54522A). A 32 bits RISC-processor kinetic spectrometer workstation was used to analyse the digitised signal. Solutions were freshly prepared before each experimental series by mixing Milli-Q water and an appropriate volume of reactants (stock solutions). The pH was adjusted using NaOH or $HClO_4$. Experiments in oxygen-free solutions were performed by bubbling nitrogen during 10 minutes before laser shots.

2.5. *Photochemical modelling*

A detailed description of the model including the relevant equations is reported in the freely available SM of several previous publications (see for instance Maddigapu et al., 2011; Minella et al., 2013; Minella et al., accepted). Moreover, a software application has been derived from the model (APEX: Aqueous Photochemistry of Environmentally-occurring Xenobiotics), which is available for free download at *http://chimica.campusnet.unito.it/do/didattica.pl/Quest?corso=7a3d* (including the User's Guide that contains a comprehensive account of model equations). Some additional model details are reported as SM.

3. *Results and Discussion*

First of all, we determined the pK_{a2} of the monoanionic form of BP-4 ($HA^- \leftrightarrows H^+ + A^{2-}$, see Figure 1 for their structures) by means of a spectrophotometric method, finding a value of 7.30±0.15 (see SM for pK_a determination). To separately study the photochemical reaction kinetics of the two species, experiments were carried out at pH 4 and 10, where HA^- and A^{2-} would respectively prevail. The solution pH was fixed with NaOH or $HClO_4$. Preliminary experiments were carried out at pH ~ 7.5, where HA^- and A^{2-} would be present in comparable amount. Photochemical modelling based on photoreactivity data at pH 7.5 suggested that direct photolysis and reaction with $^\bullet OH$ would be the main transformation processes for BP-4 in freshwater. Therefore, further investigation of the reactivity of HA^- and A^{2-} did not take into account reactions with $CO_3^{\bullet-}$, $^1O_2$ or $^3CDOM^*$. The results of the preliminary study of BP-4 reactivity at pH 7.5 by direct photolysis and reactions with $^\bullet OH$, $CO_3^{\bullet-}$, $^1O_2$ and $^3CDOM^*$ are reported as SM.

3.1. *Direct photolysis*

The transformation of BP-4 in the dark was negligible: in the absence of irradiation no more than 1% degradation was observed in 6 days, compared to 30-35% in irradiated samples.

Irradiated BP-4 (initial concentration 20 µM) at pH 4 (HA^-) had an initial reaction rate $R_{BP-4} = (1.68±0.16)\cdot10^{-11}$ M s^{-1} (first-order rate constant $k_{BP4} = (8.40±0.80)\cdot10^{-7}$ s^{-1}). At pH 10 (A^{2-}) it was $R_{BP-4} = (1.60±0.15)\cdot10^{-11}$ M s^{-1} ($k_{BP4} = (8.00±0.75)\cdot10^{-7}$ s^{-1}). In both cases the substrate was the

only radiation-absorbing component in solution, and its initial absorbed photon flux could be determined as $P_a^{BP-4} = \int_\lambda p°(\lambda)(1-10^{-\varepsilon(\lambda)bc})d\lambda$. Here, $p°(\lambda)$ is the spectral incident photon flux density, $\varep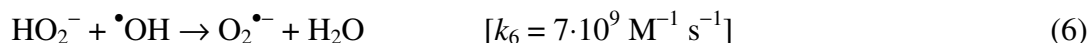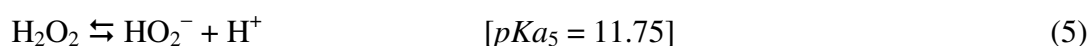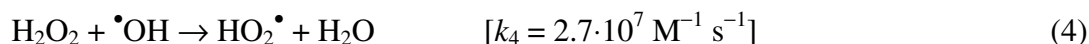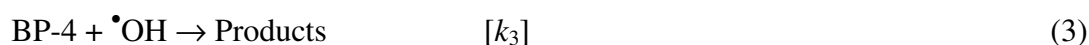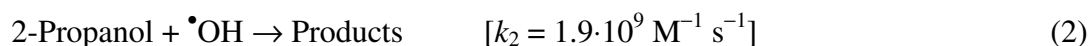silon(\lambda)$ the molar absorption coefficient of the relevant BP-4 species, b = 0.4 cm the optical path length in solution, and c = 20 μM the initial BP-4 concentration. As an approximation, the polychromatic quantum yield of BP-4 direct photolysis can be determined as $\Phi_{BP-4} = R_{BP-4}(P_a^{BP-4})^{-1}$. It is P_a^{BP-4} = (5.2±0.4)·10^{-7} Einstein L^{-1} s^{-1} at pH 4 and (2.3±0.2)·10^{-7} Einstein L^{-1} s^{-1} at pH 10. Therefore, the direct photolysis quantum yield of BP-4 is Φ_{BP-4} = (3.2±0.6)·10^{-5} at pH 4 and Φ_{BP-4} = (7.0±1.3)·10^{-5} at pH 10. Note that these values are reasonably representative of the wavelength interval where there is overlap between the spectra of lamp and BP-4 (HA$^-$ and A^{2-}). In right the same interval there is overlap between the spectra of BP-4 and of sunlight.

To get further insight into BP-4 direct photodegradation, a laser flash photolysis study was carried out at different pH values. The laser pulse wavelength was 355 nm, where both forms of BP-4 (HA$^-$ and A^{2-}) absorb radiation (see Figure 1). No transient signals could be detected at pH 10, while at pH 4 a species was formed with absorption maximum at 380 nm and a decay constant $k_{380nm} \approx 5.0\cdot10^6$ s^{-1} (see Figure 2 for the decay of the transient spectrum). The absorption maximum of this species is quite different from the typical triplet states of benzophenones (absorption maximum around 530 nm; Bensasson and Gramain, 1980). Moreover, the decay time of the transient was not affected by removal of dissolved O$_2$ from the solution under Ar stream. Negligible reactivity with oxygen has been observed with the triplet state of anthraquinone-2-sulphonate, but in that case the faster reaction with water yielded two species with clearly identifiable absorption features (Maddigapu et al., 2010). In contrast, no new radiation-absorbing species was formed with BP-4 after decay of the 380-nm signal. Therefore, spectral features and oxygen effect would exclude that the observed transient species is the triplet state of BP-4. In contrast, they would be compatible with the generation of a phenoxy radical (De Laurentiis et al., 2013) from the phenolic group of BP-4. The same 380-nm transient species was observed at pH 7.5, but no evidence of formation of solvated electrons (absorption maximum at 720 nm; Jou and Freeman, 1977) could be found under any conditions. This issue excludes a photoionisation pathway to produce the phenoxy radical, which would be consistent with the lack of radical formation at pH 10. Under these conditions, where BP-4 is under its dianionic form (A^{2-}), the only pathway that could lead the generation of phenoxy radical would be photoionisation that is not operational under UVA irradiation. On the contrary, the protonated phenolic form (HA$^-$) could produce the radical species also by homolytic breaking of the O-H bond. This pathway that often requires lower energy (such as that of the 355-nm laser photons) than photoionisation (Hornback, 2006). Comparison between laser results and steady-state irradiation experiments suggests that the direct photolysis of BP-4 at pH 4 (and at pH 7.5, data not shown) would proceed by formation of a phenoxy radical from HA$^-$. In contrast, flash photolysis experiments are silent as to the mechanism of BP-4 phototransformation at pH 10 (A^{2-} form).

3.2. Reaction with •OH

Figure 3 reports the initial transformation rates of 20 μM BP-4 at pH 4 (HA^-) and 10 (A^{2-}), upon irradiation of 1.0 mM H_2O_2 under the TL 01 lamp (see Figure 1), in the presence of variable concentration values of the •OH scavenger 2-propanol. Competition kinetics between BP-4 and 2-propanol for •OH would involve the following reactions (Buxton et al., 1988; Zellner et al., 1990; Martell et al., 1997):

$$H_2O_2 + h\nu \rightarrow 2\ {}^{\bullet}OH \qquad\qquad [R_{\bullet OH}] \qquad\qquad (1)$$

$$\text{2-Propanol} + {}^{\bullet}OH \rightarrow \text{Products} \qquad [k_2 = 1.9 \cdot 10^9\ M^{-1}\ s^{-1}] \qquad (2)$$

$$\text{BP-4} + {}^{\bullet}OH \rightarrow \text{Products} \qquad\qquad [k_3] \qquad\qquad (3)$$

$$H_2O_2 + {}^{\bullet}OH \rightarrow HO_2^{\bullet} + H_2O \qquad [k_4 = 2.7 \cdot 10^7\ M^{-1}\ s^{-1}] \qquad (4)$$

$$H_2O_2 \leftrightarrows HO_2^- + H^+ \qquad\qquad [pKa_5 = 11.75] \qquad (5)$$

$$HO_2^- + {}^{\bullet}OH \rightarrow O_2^{\bullet -} + H_2O \qquad [k_6 = 7 \cdot 10^9\ M^{-1}\ s^{-1}] \qquad (6)$$

Upon application of the steady-state approximation to •OH, one gets the following expression for the transformation rate of BP-4 (R_{BP-4}) as a function of [2-Propanol]:

$$R_{BP-4} = R_{\bullet OH} \frac{k_3[BP-4]}{k_3[BP-4] + k_2[2-\text{Propanol}] + (k_4\,\alpha_{H_2O_2} + k_6\,\alpha_{HO_2^-})\,c_{H_2O_2}} \qquad (7)$$

where $R_{\bullet OH}$ is the formation rate of •OH in equation (1), $c_{H_2O_2}$ = [H_2O_2] + [HO_2^-] = 1 mM is the total concentration of H_2O_2, and it is $\alpha_{H_2O_2}$ = [H^+] ([H^+] + Ka_5)$^{-1}$ and $\alpha_{HO_2^-}$ = Ka_5 ([H^+] + Ka_5)$^{-1}$.

The second-order rate constant values k_2, k_3 and k_4 were taken from the literature (Buxton et al., 1988; Christensen et al. 1982). The fit of the rate data of Figure 3 with equation (7) yielded k_3 = (1.87±0.31)·10^{10} M^{-1} s^{-1} at pH 4 and (8.46±0.24)·10^9 M^{-1} s^{-1} at pH 10. In both cases it was $R_{\bullet OH} \approx$ 5·10^{-9} M s^{-1}. The above values of k_3 will be used as the second-order reaction rate constants of •OH with HA^- and A^{2-}, respectively.

3.3. Reaction with $Br_2^{\bullet -}$ (laser flash photolysis)

The radical $Br_2^{\bullet -}$ was produced by 355-nm laser irradiation of the complex $Co(NH_3)_5Br^{2+}$ in the presence of 5 mM bromide, and its time evolution was monitored at 360 nm (Brigante et al. 2010). The photolysis of $Co(NH_3)_5Br^{2+}$ gives $Br^{\bullet}$, which produces $Br_2^{\bullet -}$ upon reaction with Br^- (De Laurentiis et al., 2012b). As shown above, laser irradiation at pH 4 and 7.5 yields the phenoxy radical of BP-4 that has absorption maximum at 380 nm and could potentially cause spectral interference with $Br_2^{\bullet -}$, which absorbs in the 300-420 nm range (Hug, 1981). However, the phenoxy radical is produced in relatively low amount by direct laser pulse and it disappears within 1 μs (see

8

Figure 2). In contrast, the lifetime of $Br_2^{\bullet-}$ is in the tens-μs range and the spectral interference can be easily avoided by adjusting the time window of signal monitoring. A more important interference is observed upon laser irradiation of $Co(NH_3)_5Br^{2+}$ + Br^- + BP-4, showing the formation of a species with absorption maximum at 380 nm. At mM BP-4 levels this species completely covers the $Br_2^{\bullet-}$ traces. By analogy with the reactions of $Br_2^{\bullet-}$ with phenols that yield the corresponding phenoxy radicals (Neta et al., 1988) and given the spectral similarities between the new species and the already identified phenoxy radical of BP-4, it is very likely that such a radical species is formed as well by BP-4 + $Br_2^{\bullet-}$. In this case, however, $Br_2^{\bullet-}$ would produce the phenoxy radical all along its decay. Therefore, the faster disappearance kinetics of phenoxyl compared to $Br_2^{\bullet-}$ cannot be exploited to avoid spectral interference. The only way to minimise interference was to operate at the lowest possible concentration values of BP-4, even at the cost of reducing the accuracy with which the second-order reaction rate constant between BP-4 and $Br_2^{\bullet-}$ could be measured. Figure 4 shows the Stern-Volmer plot at pH 7.5 of the pseudo-first order decay constant of $Br_2^{\bullet-}$ as a function of BP-4 concentration, by which the second-order reaction rate constant ($k_{Br_2^{-\bullet},BP-4} = (8.05 \pm 1.33) \cdot 10^8 \, M^{-1} s^{-1}$) could be derived as the slope of the fit line. The line intercept ($(9.61 \pm 0.50) \cdot 10^4 \, s^{-1}$) represents the kinetics of $Br_2^{\bullet-}$ decay in the absence of BP-4. Higher concentration values of BP-4 could not be used because of spectral interference from the phenoxy radical, which would cause a deviation from the linear trend. Some spectral interference cannot even be excluded at the highest BP-4 concentration values of Figure 4, in which case the actual second-order reaction rate constant would be somewhat higher than reported.

At pH 4, where the HA^- form of BP-4 prevails, no accurate measurement of the reaction rate constant with $Br_2^{-\bullet}$ (which would be around $10^8 \, M^{-1} s^{-1}$) could be carried out. In fact, at low BP-4 concentrations the decay constant of $Br_2^{-\bullet}$ was not sufficiently differentiated from that observed without BP-4. Higher values of BP-4 concentration could not be used because of spectral interference. At pH 10, high spectral interference prevented any accurate measurement of the decay of $Br_2^{\bullet-}$. The higher reaction rate constant of $Br_2^{\bullet-}$ with BP-4 at pH 7.5 compared with pH 4 is most likely accounted for by the fact that $Br_2^{\bullet-}$ reacts by electron extraction, which is considerably more efficient with phenolates (such as A^{2-}) than with phenols (such as HA^-) (Neta et al., 1988). The very elevated formation of the phenoxy radical of BP-4 at pH 10 would also account for the spectral interference, which prevented the measurement of the reaction rate constant between BP-4 (A^{2-} form) and $Br_2^{\bullet-}$.

3.4. *Effect of Br⁻ on BP-4 transformation upon nitrate photolysis*

Nitrate as photochemical $^\bullet OH$ source could be involved into the transformation of BP-4 in aqueous solution. The process could be inhibited by $^\bullet OH$ scavengers, most notably DOM in freshwater and bromide in saltwater. Figure 5 reports the trend of BP-4 transformation rate (R_{BP-4}, initial BP-4 concentration 20 μM) upon irradiation of 10 mM nitrate (TL 01 lamp, Figure 1), as a function of bromide at pH 7.5. Despite the role of Br^- as $^\bullet OH$ scavenger (a process that yields $Br_2^{\bullet-}$ as key

intermediate; Buxton et al., 1988) and the fact that $Br_2^{\bullet-}$ is considerably less reactive than $^{\bullet}OH$, one observes a practically constant degradation rate till 1 mM bromide and a considerable increase afterwards.

Such an increase could be linked with the solvent-cage reactivity of nitrate upon photolysis (Bouillon and Miller, 2005; Nissenson et al., 2010; Vione et al., 2011b). Indeed, irradiation splits the nitrate ion into photofragments ($O^{\bullet-}$ and $^{\bullet}NO_2$) that are initially surrounded by water molecules (the so-called solvent cage). Cage fragments can either recombine or diffuse into the solution bulk ($O^{\bullet-}$ would also be protonated to $^{\bullet}OH$), and the two processes are in competition. In the presence of $^{\bullet}OH$ scavengers at sufficiently high concentration, a further process could be the reaction between scavenger and cage fragments (most notably $O^{\bullet-}$ or $^{\bullet}OH$ that are significantly more reactive than $^{\bullet}NO_2$; Buxton et al., 1988; Neta et al., 1988). Such a reaction would oxidise the scavengers and, by consuming $O^{-\bullet}/^{\bullet}OH$, it would also inhibit the cage recombination process (Nissenson et al., 2010).

If the scavenger involved is bromide, there would be oxidation to $Br^{\bullet}$ followed by further reaction with bromide to yield the reactive species $Br_2^{\bullet-}$ (Buxton et al., 1988; Neta et al., 1988; Bouillon and Miller, 2005). Note that $Br_2^{\bullet-}$ would be formed from bromide both upon scavenging of cage $O^{\bullet-}/^{\bullet}OH$, and upon reaction with $^{\bullet}OH$ in the solution bulk (see Scheme 1). By combination of the two processes, and because of inhibition of cage recombination between $O^{\bullet-}/^{\bullet}OH$ and $^{\bullet}NO_2$, the formation rate of $Br_2^{\bullet-}$ at high bromide would be higher than the formation rate of $^{\bullet}OH$ without bromide. The formation of a less reactive species in higher amount can have variable impact depending on substrate reactivity: transformation of compounds that are unreactive toward $Br_2^{\bullet-}$ would be inhibited by bromide, while transformation of sufficiently reactive compounds could be enhanced (Das et al., 2009). The results shown in Figure 5 suggest that BP-4 would be fairly reactive toward $Br_2^{\bullet-}$, coherently with the laser flash photolysis results. A kinetic model able to account for the trend of R_{BP-4} *vs.* bromide concentration includes the following reactions:

$$NO_3^- + h\nu + H^+ \rightarrow [^{\bullet}OH + {}^{\bullet}NO_2]_{cage} \qquad [R_8] \qquad (8)$$

$$[^{\bullet}OH + {}^{\bullet}NO_2]_{cage} \rightarrow NO_3^- + H^+ \qquad [k_9] \qquad (9)$$

$$[^{\bullet}OH + {}^{\bullet}NO_2]_{cage} \rightarrow {}^{\bullet}OH + {}^{\bullet}NO_2 \qquad [k_{10}] \qquad (10)$$

$$[^{\bullet}OH + {}^{\bullet}NO_2]_{cage} + Br^- \rightarrow Br^{\bullet} + OH^- + {}^{\bullet}NO_2 \qquad [k_{11}] \qquad (11)$$

$$^{\bullet}OH + Br^- \rightarrow OH^- + Br^{\bullet} \qquad [k_{12}] \qquad (12)$$

$$Br^{\bullet} + Br^- \rightarrow Br_2^{\bullet-} \qquad [k_{13}] \qquad (13)$$

$$^{\bullet}OH + BP\text{-}4 \rightarrow Products \qquad [k_{14}] \qquad (14)$$

$$Br_2^{\bullet-} + BP\text{-}4 \rightarrow Products \qquad [k_{15}] \qquad (15)$$

$$Br_2^{\bullet-} \rightarrow Other\ species \qquad [k_{16}] \qquad (16)$$
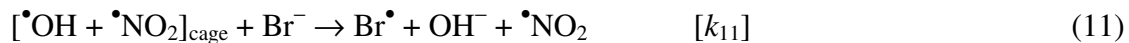
Note that equation (16) was given a pseudo-first order form to allow a manageable solution of the kinetic system. The radical $Br_2^{\bullet-}$ could for instance be transformed by disproportionation in aqueous solution (Neta et al., 1988), but inclusion of the reaction between two $Br_2^{-\bullet}$ into the model would introduce a quadratic term in reaction rate equations, and it would prevent a non-numerical

solution of the already complex kinetic system. By applying the steady-state approximation to [$^\bullet$OH + $^\bullet$NO$_2$]$_{cage}$, $^\bullet$OH, Br$^\bullet$ and Br$_2$$^{\bullet-}$, from reactions (8)-(16) one gets the following expression for R_{BP-4} as a function of bromide concentration:

$$R_{BP-4} = R_8 \frac{[Br^-]^2(k_{11}k_{15}k_{12}[BP4]) + [Br^-](k_{11}k_{14}k_{15}[BP4]^2 + k_{10}k_{12}k_{15}[BP4]) + k_{10}k_{14}k_{15}[BP4]^2 + k_{10}k_{14}k_{16}[BP4]}{(k_9 + k_{10} + k_{11}[Br^-])(k_{12}[Br^-] + k_{14}[BP4])(k_{16} + k_{15}[BP4])} \quad (17)$$

On the basis of literature data (Buxton et al., 1988; Neta et al., 1988; Vione et al., 2011b) one can fix $k_9 = 5 \cdot 10^8$ s^{-1}, $k_{10} = 1 \cdot 10^8$ s^{-1}, $k_{12} = 1.1 \cdot 10^{10}$ M^{-1} s^{-1} and $k_{13} = 1.0 \cdot 10^{10}$ M^{-1} s^{-1}. From our laser flash photolysis results at pH 7.5 one gets $k_{15} = (8.05 \pm 1.33) \cdot 10^8$ M^{-1} s^{-1}, while the reaction rate constant between BP-4 and $^\bullet$OH at pH 7.5 would be intermediate between those of HA$^-$ and A^{2-} ($k_{14} \sim 1.4 \cdot 10^{10}$ M^{-1} s^{-1}). To obtain the right ratio (0.3) between the initial transformation rate of BP-4 without bromide and that with 0.3 M bromide, one has to assume $k_{11} \sim 3 \cdot 10^9$ M^{-1} s^{-1}. With these fixed values and with floating R_8 and k_{16}, the fit of the experimental data of R_{BP-4} *vs.* [Br$^-$] with equation (17) is reported as the dashed curve in Figure 5. From data fit one obtains $R_8 = (2.6 \pm 0.4) \cdot 10^{-9}$ M s^{-1}, while k_{16} (around $5 \cdot 10^3$ s^{-1}) is affected by a large error. The latter issue implies that data fit is little sensitive to the actual value of k_{16}.

If the cage reaction (11) of bromide is neglected (which is equivalent to placing $k_{11} = 0$ in equation 17), the kinetic system foresees the trend that is shown as a solid curve in Figure 5. Under such circumstances one would expect a slight inhibition by bromide of BP-4 degradation upon nitrate photolysis. The fact that bromide enhances BP-4 transformation suggests that the formation rate of Br$_2$$^{\bullet-}$ with bromide is higher than the formation rate of $^\bullet$OH without bromide, which is consistent with the hypothesised cage reaction. Note, however, that an almost insignificant effect of bromide is expected under typical environmental conditions (up to 1 mM Br$^-$ in seawater; Jiang et al., 2009), independently of the occurrence of the cage reaction. Therefore, the cited process would have limited environmental importance, with the likely exception of hypersaline system that can be present in some arid environments because of water evaporation (Leroy et al., 2006). However, additional Br$_2$$^{\bullet-}$ sources such as the oxidation of bromide by ^{3}CDOM* (Graetzel and Halmann, 1990; De Laurentiis et al., 2012b) might play an important role in the environmental phototransformation of BP-4 (*vide infra*).

3.5. *Modelling of BP-4 phototransformation kinetics in surface waters.*

It is possible to get insight into the photochemical persistence of BP-4 in surface waters by using the APEX software, with input data (photolysis quantum yields and reaction rate constants with $^\bullet$OH and Br$_2$$^{\bullet-}$) obtained in the present work. A preliminary study (see SM) showed that reactions with CO$_3$$^{\bullet-}$, ^{1}O$_2$ and ^{3}CDOM* would play a minor to negligible role in the environmental transformation of BP-4. Under conditions where bromide is unimportant, direct photolysis and reaction with $^\bullet$OH would thus be the main phototransformation pathways of BP-4. At the typical pH

values of surface waters, BP-4 would be present as a mixture of the monoanion (HA$^-$) and the dianion (A^{2-}) depending on pH (pK$_{a2}$ = 7.3 as determined in this work, see SM). Reaction with $^\bullet$OH is faster in the case of HA$^-$, while the photolysis quantum yield is significantly higher for A^{2-}. Moreover, while HA$^-$ mostly absorbs sunlight in the UVB region, the absorption of A^{2-} mainly takes place in the UVA and it is also extended into the visible (see Figure 1). Therefore, the different photochemical reactivity of HA$^-$ and A^{2-} could influence the phototransformation kinetics of BP-4 as a function of pH. The transformation of the two species was calculated separately in the model, based on reaction rate constants with $^\bullet$OH, photolysis quantum yields and absorption spectra. The overall rate constant of BP-4 phototransformation was derived from the weighted contributions of HA$^-$ and A^{2-} at each relevant pH value, as $k_{BP-4} = \alpha_{HA^-} \, k_{HA^-} + \alpha_{A^{2-}} \, k_{A^{2-}}$, where $\alpha_{HA^-} = [\text{H}^+] \, ([\text{H}^+] + K_{a2})^{-1}$ and $\alpha_{A^{2-}} = K_{a2} \, ([\text{H}^+] + K_{a2})^{-1}$.

Figure 6 reports the modelled pseudo-first order transformation rate constant of BP-4 as a function of some of the environmental parameters that are most significant from an environmental point of view: pH and depth d (6a), DOC value (dissolved organic carbon, which measures DOM) (6b), and nitrate concentration (6c). Note that when not set as variables, water chemistry parameters were as follows: 5 m depth, 3 mg C L^{-1} DOC, 0.1 mM nitrate, 1 µM nitrite, and 1 mM inorganic carbon. The pH trend gives insight into the relative transformation kinetics of HA$^-$ and A^{2-}, where the former is degraded faster than the latter upon reaction with $^\bullet$OH, and the opposite holds for direct photolysis. In most cases the dianionic form (A^{2-}) is photodegraded faster compared to the monoanionic one (HA$^-$), by a factor of up to ~3 under favourable conditions (high d and low nitrate or nitrite, which favour direct photolysis compared to $^\bullet$OH). There would be exceptions, however, especially at low DOC where the $^\bullet$OH process is strongly favoured and HA$^-$ is expected to undergo faster degradation than A^{2-}.

Figure 6a shows that BP-4 phototransformation gets slower when depth is higher. This is due to the fact that the bottom layers of a deeper water body are poorly illuminated by sunlight, while shallower environments are more thoroughly illuminated. Moreover, the relative importance of $^\bullet$OH reaction $vs.$ direct photolysis increases with depth in the case of HA$^-$. This happens because nitrite and CDOM (important $^\bullet$OH sources) significantly absorb sunlight at UVA and visible wavelengths, while the direct photolysis of HA$^-$ is mostly triggered by UVB radiation. UVA and visible radiations penetrate more deeply into the water column compared to UVB, thus $^\bullet$OH reactions are still active at depths where HA$^-$ photolysis becomes insignificant. The opposite situation is predicted for A^{2-}, because of its significant radiation absorption in the UVA and visible regions.

Figure 6b shows that the rate constant of BP-4 photodegradation decreases with increasing DOC, because of combination of $^\bullet$OH scavenging by DOM and competition for sunlight irradiance between CDOM and BP-4. The former effect is more important, and the relative role of $^\bullet$OH reaction $vs.$ direct photolysis decreases with increasing DOC for both HA$^-$ and A^{2-}. The main consequence is that the transformation rate constant decreases with pH at low DOC (faster transformation of HA$^-$ compared to A^{2-}, because of faster reaction with $^\bullet$OH that is the main

pathway) and increases with pH at high DOC (faster transformation of A^{2-} because its direct photolysis is faster than for HA^-).

Figure 6c shows that BP-4 phototransformation becomes faster with increasing nitrate concentration, due to enhanced $^\bullet$OH photoproduction. Similar results are observed with increasing nitrite concentration (data not shown).

Figure 6 suggests that BP-4 would have half-life times in the order of days to weeks in sunlit, shallow freshwaters under mid-latitude summertime conditions. Therefore, direct photolysis and $^\bullet$OH reaction are potentially very important transformation pathways for BP-4 in surface-water environments.

In addition to WWTP discharge, the use of BP-4 in sunbathing lotions enables a direct emission pathway to surface waters and most notably to saltwater environments. Under such circumstances, reactivity between BP-4 and $Br_2^{\bullet-}$ might become important. The predictions of the photochemical model have been verified in estuarine (brackish) waters (Maddigapu et al., 2011; Sur et al., 2012) but not in seawater, thus any extrapolation to the latter case should be taken with great care. Despite these limitations, it is still interesting to get some insight into the possible effect of bromide on BP-4 phototransformation. First of all, $Br_2^{\bullet-}$ can be produced upon bromide oxidation by both $^\bullet$OH (rate constant $k_{^\bullet OH,Br^-} = 1.1 \cdot 10^{10}$ M^{-1} s^{-1}; Buxton et al., 1988) and ^{3}CDOM* (rate constant $k_{^3CDOM*,Br^-} = 3 \cdot 10^9$ M^{-1} s^{-1}; De Laurentiis et al., 2012b). The reaction rate constant between $Br_2^{\bullet-}$ and DOM is $k_{DOM,Br_2^{\bullet-}} \sim 3 \cdot 10^2$ L (mg C)$^{-1}$ s^{-1} (De Laurentiis et al., 2012b), and $Br_2^{-\bullet}$ could undergo further deactivation processes. The intercept of the linear fit to the laser data reported in Figure 4 suggests a possible value for the pseudo-first order decay constant of $Br_2^{\bullet-}$ alone ($k_{Br_2^{\bullet-}} = (9.61 \pm 0.50) \cdot 10^4$ s^{-1}). The fit with equation (17) of the steady irradiation data reported in Figure 5 suggests a much lower (over 10 fold) estimate for the same pseudo-first order rate constant (k_{16}), although with considerable uncertainty. The difference might be due to the fact that $Br_2^{\bullet-}$ partially disappears by disproportion that is a second-order process, and the amount of $Br_2^{\bullet-}$ produced by the laser pulse is probably much higher compared to steady irradiation. Anyway, as a conservative estimate we took the former and higher value for $Br_2^{-\bullet}$ decay: if the actual disappearance of $Br_2^{\bullet-}$ is slower, the steady-state $[Br_2^{\bullet-}]$ is higher and the related processes are more important than predicted. Based on the above assumptions and applying the steady-state approximation to $Br_2^{\bullet-}$, the first-order rate constant of BP-4 transformation upon reaction with $Br_2^{\bullet-}$ can be expressed as follows:

$$k_{BP-4}^{Br_2^{\bullet-}} = k_{BP-4,Br_2^{\bullet-}} \cdot [Br_2^{-\bullet}] = k_{BP-4,Br_2^{\bullet-}} \cdot \frac{k_{^\bullet OH,Br^-}[^\bullet OH] + k_{^3CDOM*,Br^-}[^3CDOM*]}{k_{DOM,Br_2^{\bullet-}}DOC + k_{Br_2^{\bullet-}}} \tag{18}$$

where $[^\bullet OH]$ and $[^3CDOM*]$ are derived from the model, also taking into account the respective reactions with bromide, and $k_{BP-4,Br_2^{\bullet-}}$ is the second-order reaction rate constant between BP-4 and $Br_2^{\bullet-}$. For this rate constant we took the value of $(8.05 \pm 1.33) \cdot 10^8$ $M^{-1} s^{-1}$ determined by laser flash

photolysis at pH 7.5 (see section 3.3). The overall pseudo-first order degradation rate constant of BP-4 is given by the sum of $k_{BP-4}^{Br_2^{\bullet-}}$ plus the corresponding quantities referred to $^{\bullet}OH$ reaction and direct photolysis. In the latter two cases, a mixed contribution of the two forms of BP-4 (HA$^-$ and A^{2-}) in comparable amount was taken into account.

Figure 7 shows the modelled pseudo-first order rate constant of BP-4 phototransformation ($k_{tot} = k_{BP-4}^{Br_2^{\bullet-}} + k_{BP-4}^{\bullet OH} + k_{BP-4}^{Phot}$) as a function of DOC and bromide. The decrease of k_{tot} with increasing DOC is mostly due to competition for irradiance between CDOM and BP-4, which decreases the rate constant of BP-4 direct photolysis. Increasing DOC also implies higher scavenging of $^{\bullet}OH$ by DOM but, at the same time, higher generation of $Br_2^{\bullet-}$ by $^3CDOM^* + Br^-$. Interestingly, increasing bromide would inhibit the phototransformation of BP-4 at low DOC and enhance it at high DOC. At low DOC the pathway of $Br_2^{\bullet-}$ production by $^3CDOM^*$ has limited importance and the main effect of bromide is to scavenge $^{\bullet}OH$ and replace it with the less reactive species $Br_2^{\bullet-}$. In contrast, at high DOC the reaction between $^3CDOM^*$ and bromide to yield $Br_2^{\bullet-}$ enhances the degradation of BP-4. For instance, under high-DOC and high-bromide conditions, about two thirds of BP-4 phototransformation is predicted to take place upon reaction with $Br_2^{\bullet-}$. Therefore, despite the unavoidable limitations and approximations linked with the treatment of $Br_2^{\bullet-}$ reactivity, there is evidence that this species may potentially play an important role in BP-4 phototransformation in bromide-rich environments.

4. *Conclusions*

- The two forms of BP-4 that prevail under surface-water conditions (HA$^-$ and A^{2-}, with $pK_{a2} = 7.30\pm0.15$) have respective second-order reaction rate constants with $^{\bullet}OH$ of $(1.87\pm0.31)\cdot10^{10}$ M^{-1} s^{-1} and $(8.46\pm0.24)\cdot10^{9}$ M^{-1} s^{-1}, and direct photolysis quantum yields of $(3.2\pm0.6)\cdot10^{-5}$ and $(7.0\pm1.3)\cdot10^{-5}$, respectively.

- The direct photolysis of the HA$^-$ form, as studied by laser flash photolysis, would likely proceed by homolysis of the phenolic O-H bond to produce the corresponding phenoxy radical. Photoionisation of BP-4 by near-UV radiation to produce aquated e$^-$ can be excluded.

- BP-4 reacts significantly with $Br_2^{\bullet-}$, by which it is oxidised to the phenoxy radical. The second-order reaction rate constant at pH 7.5 is $k_{Br_2^{\bullet-},BP-4} = (8.05\pm1.33)\cdot10^{8}\,M^{-1}\,s^{-1}$. There is evidence that the reaction of HA$^-$ with $Br_2^{-\bullet}$ is somewhat slower than for A^{2-}.

- In surface freshwaters under sunlight illumination, the phototransformation of BP-4 would mainly take place upon direct photolysis and $^{\bullet}OH$ reaction. Under most conditions the A^{2-} form would be degraded faster compared to HA$^-$ because of faster direct photolysis, but there are exceptions. Most notably, in very DOM-poor waters the $^{\bullet}OH$ process would be the prevailing transformation route of BP-4, and faster degradation is predicted for HA$^-$ that reacts faster with $^{\bullet}OH$ compared to A^{2-}.

- Reaction between BP-4 and $Br_2^{\bullet-}$ could be important in bromide-rich environments, in particular in the presence of elevated DOC values, where the reaction between $^3CDOM^*$ and bromide could be an important $Br_2^{\bullet-}$ source.

References

Alanko, K., Jolanki, R., Estlander, T., Kanerva, L., 2001. Occupational allergic contact dermatitis from benzophenone-4 in hair-care products. Contact Dermatitis 44, 188.

Albinet, A., Minero, C., Vione, D., 2010. Phototransformation processes of 2,4-dinitrophenol, relevant to atmospheric water droplets. Chemosphere 80, 753-758.

Bensasson, R. V., Gramain, J. C., 1980. Benzophenone triplet properties in acetonitrile and water. Reduction by lactams. Journal of the Chemical Society, Faraday Transactions 1: Physical Chemistry in Condensed Phases 76, 1800–1810.

Boreen, A. L., Arnold, W. A., McNeill, K., 2003. Photodegradation of pharmaceuticals in the aquatic environment: A review. Aquatic Sciences 65, 320-341.

Bouillon, R. C., Miller, W. L., 2005. Photodegradation of dimethyl sulfide (DMS) in natural waters: laboratory assessment of the nitrate-photolysis-induced DMS oxidation. Environmental Science and Technology 39, 9471-9477.

Brigante, M., Charbouillot, T., Vione, D., Mailhot, G., 2010. Photochemistry of 1-nitronaphthalene: A potential source of singlet oxygen and radical species in atmospheric waters. Journal of Physical Chemistry A 114, 2830-2836.

Buxton, G.V., Greenstock, C.L., Helman, W.P., Ross, A.B., 1988. Critical review of rate constants for reactions of hydrated electrons, hydrogen atoms and hydroxyl radicals ($^\bullet OH/O^{-\bullet}$) in aqueous solution. Journal of Physical and Chemical Reference Data 17, 1027-1284.

Canonica, S., Urs, J., Konrad, S., Hoigné, J., 1995. Transformation kinetics of phenols in water: Photosensitization by dissolved natural organic material and aromatic ketones. Environmental Science and Technology 29, 1822-1831.

Canonica, S., Freiburghaus, M., 2001. Electron-rich phenols for probing the photochemical reactivity of freshwaters. Environmental Science and Technology 35, 690-695.

Canonica, S., Kohn, T., Mac, M., Real, F.J., Wirz, J., Von Gunten, U., 2005. Photosensitizer method to determine rate constants for the reaction of carbonate radical with organic compounds. Environmental Science and Technology 39, 9182-9188.

Caruana, D., McPherson, T., Cooper, S., 2011. Allergic contact dermatitis caused by benzophenone-4 in a printer. Contact Dermatitis 64, 158-184.

Christensen, H., Sehested, K., Corfitzen, H., 1982. Reactions of hydroxyl radicals with hydrogen peroxide at ambient and elevated temperatures. Journal of Physical Chemistry 86, 1588 – 1590.

Das, R., Dutta, B.K., Maurino, V., Vione, D., Minero, C., 2009. Suppression of inhibition of substrate photodegradation by scavengers of hydroxyl radicals: the solvent-cage effect of bromide on nitrate photolysis. Environmental Chemistry Letters 7, 337-342.

De Coster, S., van Larebeke, N., 2012. Endocrine-disrupting chemicals: Associated disorders and mechanisms of action. Journal of Environmental and Public Health, article 713696.

De Laurentiis, E., Chiron, S., Kouras-Hadef, S., Richard, C., Minella, M., Maurino, V., Minero, C., Vione, D., 2012a. Photochemical fate of carbamazepine in surface freshwaters: Laboratory measures and modelling. Environmental Science and Technology 46, 8164-8173.

De Laurentiis, E., Minella, M., Maurino, V., Minero, C., Mailhot, G., Sarakha, M., Brigante, M., Vione, D., 2012b. Assessing the occurrence of the dibromide radical ($Br_2^{-\bullet}$) in natural waters; Measures of triplet-sensitised formation, reactivity, and modelling. Science of the Total Environment 439, 299-306.

De Laurentiis, E., Maurino, V., Minero, C., Vione, D., Mailhot, M., Brigante, M., 2013. Could triplet-sensitised transformation of phenol compounds represent a source of fulvic-like substances in natural waters? Chemosphere 90, 881-884.

Díaz-Cruz, M. S., Barceló, D., 2009. Chemical analysis and ecotoxicological effects of organic UV-absorbing compounds in aquatic ecosystems. Trends in Analytical Chemistry 28, 708-717.

Fent, K., Zenker, A., Rapp, M., 2010. Widespread occurrence of estrogenic UV-filters in aquatic ecosystems in Switzerland. Environmental Pollution 158, 1817-1824.

Fent, K., Kunz, P., Zenker, A., Rapp, M., 2010a. A tentative environmental risk assessment of the UV filters 3-(4-methylbenzylidene-camphor), 2-ethyl-hexyl-4-trimethoxycinnamate, benzophenone-3-, benzophenone-4 and 3-benzilidene camphor. Marine Environmental Research 69, S4-S6.

Gerecke, A. C., Canonica, S., Müller, S. R., Scharer, M., Schwarzenbach, R. P., 2001. Quantification of dissolved natural organic matter (DOM)-mediated phototransformation of phenylurea herbicides in lakes. Environmental Science and Technology 35, 3915-3923.

Graetzel, M., Halmann, M., 1990. Photosensitized oxidation of bromide in Dead Sea water. Marine Chemistry 29, 169-182.

Hornback, J. M., 2006. Organic chemistry, second edition. Thomson books.

Hug GL. Optical spectra of non-metallic inorganic transient species in aqueous solution. NSRDS-NBS 69, US (Washington DC): Government Printing Office.

Inui, M., Adachi, T., Takenaka, S., Inui, H., Nakazawa, M., Ueda, M., Watanabe, H., Mori, C., Iguchi, T., Miyatake, K., 2003. Effect of UV-screens and preservatives on vitellogenin and choriogenin production in male medaka (Oryzias latipes). Toxicology 194, 43-50.

Jiang, X. L., Lim, L. W., Takeuchi, T., 2009. Determination of trace inorganic anions in seawater samples by ion chromatography using silica columns modified with cetyltrimethylammonium ion. Analytical and Bioanalytical Chemistry 393, 387-391.

Jou, F. Y., Freeman, G R., 1977. Shapes of optical spectra of solvated electrons. Effect of pressure. Journal of Physical Chemistry 81, 909-915.

Kunz, P., Fent, K., 2006. Multiple hormonal activities of UV filters and comparison of *in vivo* and *in vitro* estrogenic activity of ethyl-4-aminobenzoate in fish. Aquatic Toxicology 79, 305-324.

Kunz, P.Y., Galicia, H.F., Fent, K., 2006. Comparison of *in vitro* and *in vivo* estrogenic activity of UV filters in fish. Toxicological Science 90, 349-361.

Leroy, S. A. G., Marret, F., Giralt, S., Bulatov, S. A., 2006. Natural and anthropogenic rapid changes in the Kara-Bogaz Gol over the last two centuries reconstructed from palynological analyses and a comparison to instrumental records. Quaternary International 150, 52-70.

Maddigapu, P. R., Minero, C., Maurino, V., Vione, D., Brigante, M., Mailhot, G., 2010. Enhancement by anthraquinone-2-sulphonate of the photonitration of phenol by nitrite: Implication for the photoproduction of nitrogen dioxide by coloured dissolved organic matter in surface waters. Chemophere 81, 1401-1406.

Maddigapu, P. R., Minella, M., Vione, D., Maurino, V., Minero, C., 2011. Modeling phototransformation reactions in surface water bodies: 2,4-Dichloro-6-nitrophenol as a case study. Environmental Science and Technology 45, 209-214.

Martell, A. E., Smith, R. M., Motekaitis, R. J., 1997. Critically selected stability constants of metal complexes database. Version 4.0.

Minella, M., Rogora, M., Vione, D., Maurino, V., Minero, C., 2011. A model approach to assess the long-term trends of indirect photochemistry in lake water. The case of Lake Maggiore (NW Italy). Science of the Total Environment 409, 3463–3471.

Minella, M., De Laurentiis, E., Buhvestova, O., Haldna, M., Kangur, K., Maurino, V., Minero, C., Vione, D., 2013. Modelling lake-water photochemistry: Three-decade assessment of the steady-state concentration of photoreactive transients ($^\bullet$OH, $CO_3^{-\bullet}$ and $^3CDOM^*$) in the surface water of polymictic Lake Peipsi (Estonia/Russia). Chemosphere 90, 2589-2596.

Minella, M., Maurino ,V., Minero, C., Vione., D., accepted. Modelling photochemical transformation of emerging organic pollutants in surface waters: Effect of water level fluctuations following outflow or evaporation, relevant to arid and semi-arid environments. International Journal of Environmental Analytical Chemistry.

Negreira, N., Rodriguez, I., Ramil, M., Rubì, E., Cela, R., 2009. Solid-phase extraction followed by liquid chromatography-tandem mass spectrometry for the determination of hydroxylated benzophenone UV absorbers in environmental water samples. Analytica Chimica Acta 654, 162-170.

Neta, P., Huie, R. E., Ross, A. B., 1988. Rate constants for reactions of inorganic radicals in aqueous solution, Journal of Physical and Chemical Reference Data 17, 1027-1034.

Nissenson, P., Dabdub, D., Das, R., Maurino, V., Minero, C., Vione, D., 2010. Evidence of the water cage effect on the photolysis of NO_3^- and $FeOH^{2+}$. Implications of this effect and of H_2O_2 surface accumulation on photochemistry at the air–water interface of atmospheric droplets. Atmospheric Environment 44, 4859–4866.

Page, S. E., Arnold, W. A., McNeill, K., 2011. Assessing the contribution of free hydroxyl radical in organic matter-sensitized photohydroxylation reactions. Environmental Science and Technology 45, 2818-2825.

Poiger, T., Buser, H. R., Balmer, M. E., Bergqvit, P. A., Muller, M. D. 2004. Occurrence of UV filter compounds from sunscreens in surface waters: Regional mass balance in two Swiss lakes. Chemosphere 55, 951-963.

Sur, B., De Laurentiis, E., Minella, M., Maurino, V., Minero, C., Vione, D., 2012. Photochemical transformation of 2-nitro-4-chlorophenol in surface waters: Laboratory and model assessment of the degradation kinetics, and comparison with field data. Science of the Total Environment 426, 296-303.

Vione, D., Maddigapu, P. R., De Laurentiis, E., Minella, M., Pazzi, M., Maurino, V., Minero, C., Kouras, S., Richard, C., 2011a. Modelling the photochemical fate of ibuprofen in surface waters. Water Research 45, 6725-6736.

Vione, D., Sur, B., Dutta, B. K., Maurino, V., Minero, C., 2011b. On the effect of 2-propanol on phenol photonitration upon nitrate photolysis. Journal of Photochemistry and Photobiology A: Chemistry 224, 68-70.

Wick, A., Fink, G., Ternes, T., 2010. Comparison of electrospray ionization and atmospheric pressure chemical ionization for multi-residue analysis of biocides, UV-filters and benzothiazoles in aqueous matrices and activated sludge by liquid chromatography–tandem mass spectrometry. Journal of Chromatography A 1217, 2088–2103.

Zellner, R., Exner, M., Herrmann, H., 1990. Absolute OH quantum yields in the laser photolysis of nitrate, nitrite and dissolved H_2O_2 at 308 and 351 nm in the temperature range 278-353 K. Journal of Atmospheric Chemistry 10, 411-425.
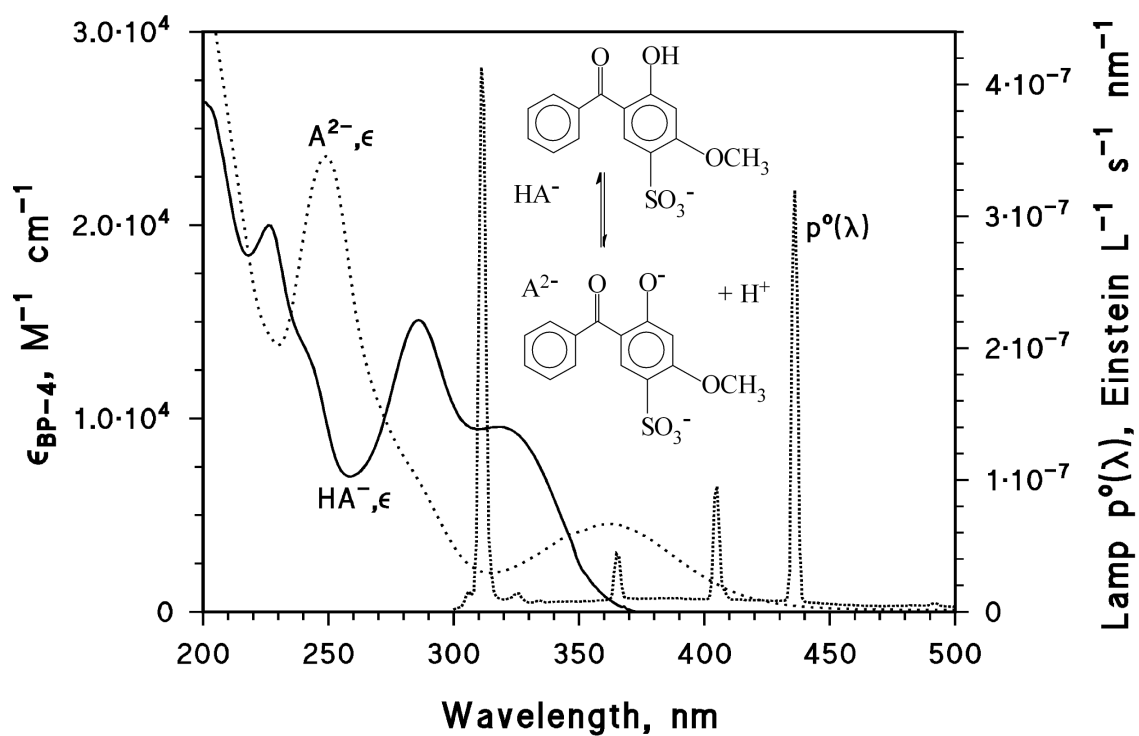
Figure 1. Absorption spectra (molar absorption coefficients) of the singly and doubly deprotonated forms of BP-4 (HA^- and A^{2-}, respectively). The structures of HA^- and A^{2-} are also reported.
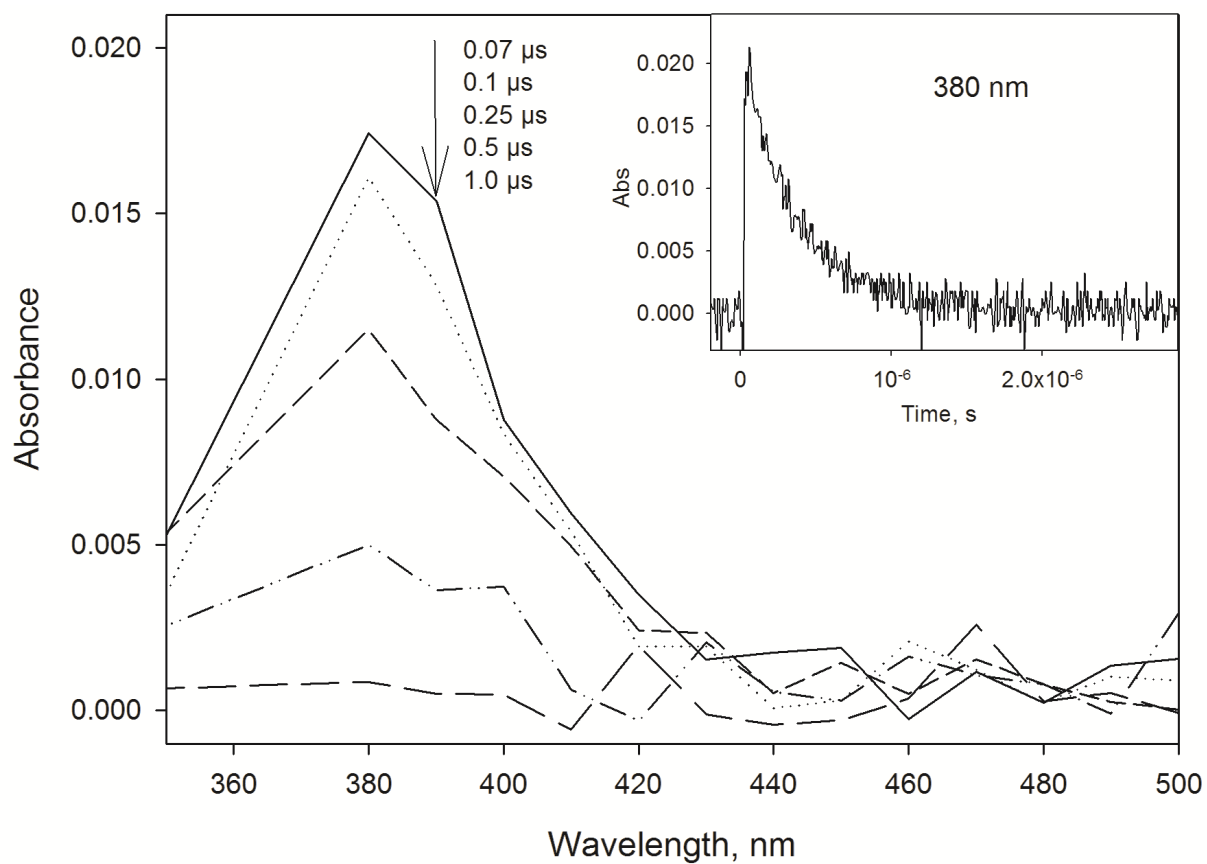
Figure 2. Time trend of the transient spectrum obtained upon laser-pulse excitation (355 nm, 90mJ) of 0.5 mM BP-4 at pH 4. The insert shows the time trend of the signal at 380 nm.
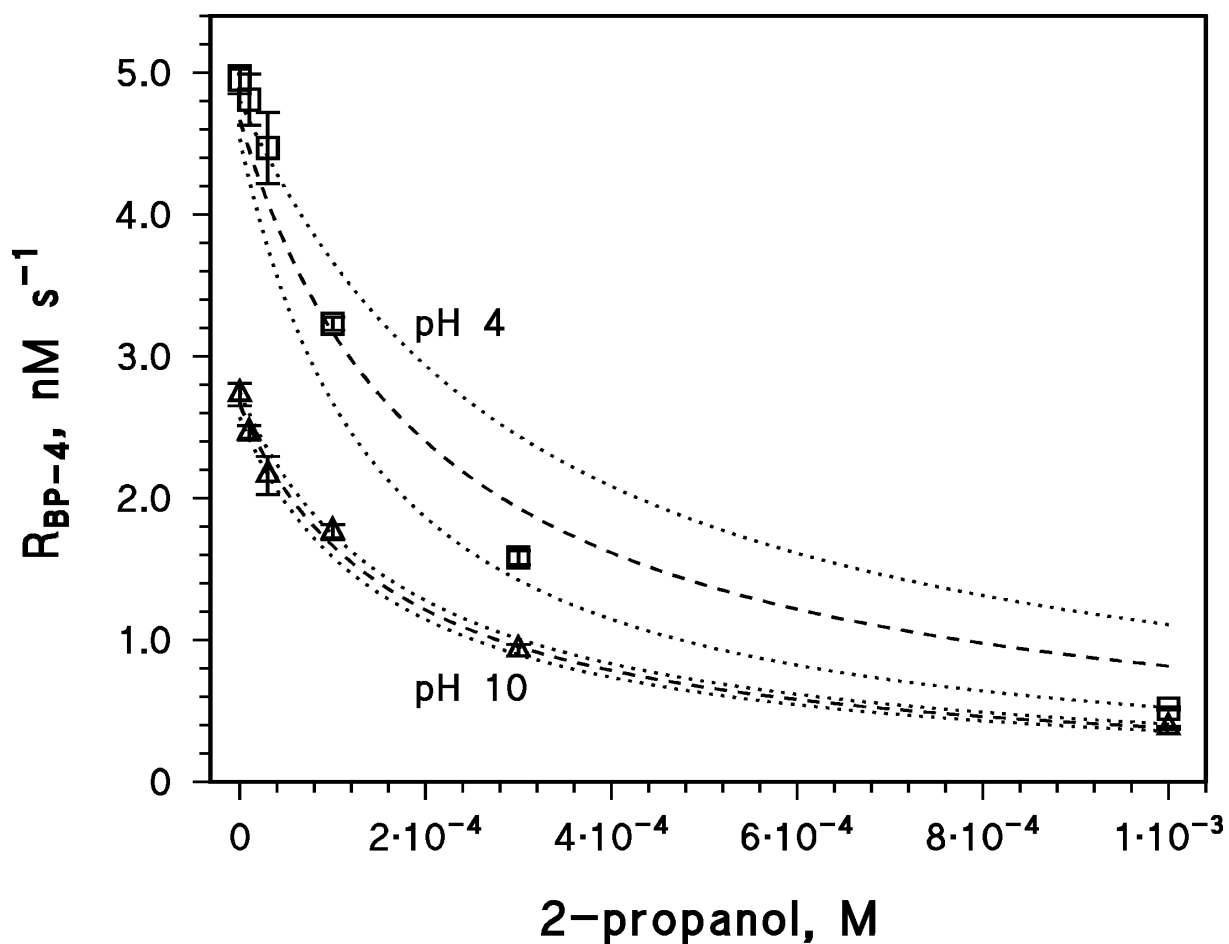
Figure 3. Initial BP-4 transformation rate (R_{BP-4}) as a function of the concentration of 2-propanol, upon irradiation of 1 mM H_2O_2 at pH 4 and 10. The error bands represent $\mu\pm\sigma$, the dashed curves are the fits of experimental rate data with equation (7), the dotted ones are the 95% confidence limits of the fit.
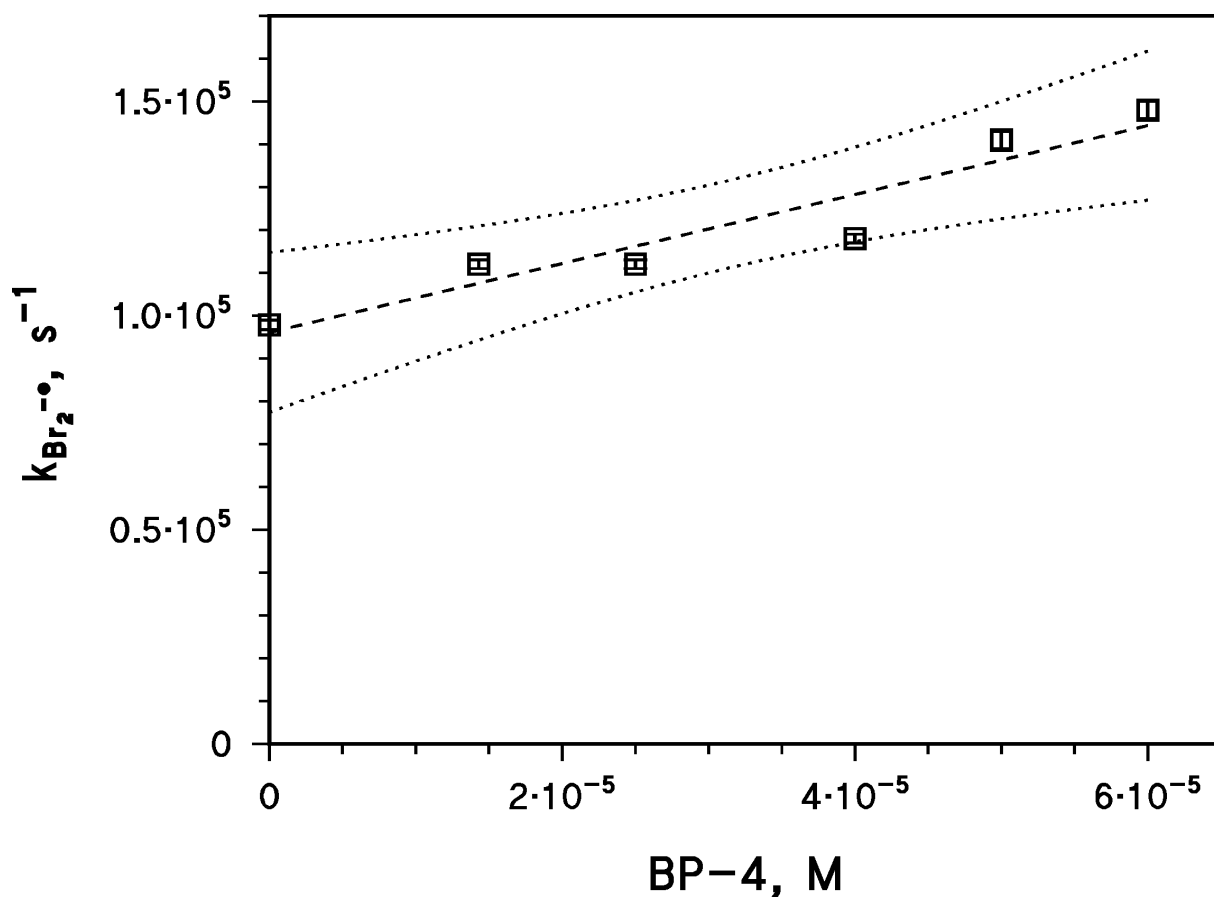
Figure 4. Trend of the pseudo-first order rate constant of $Br_2^{-\bullet}$ decay ($k_{Br_2^{-\bullet}}$) as a function of BP-4 concentration (Stern-Volmer plot). Laser pulse at 355 nm, pulse energy 60 mJ, pH 7.5. The dashed line is the linear fit, the dotted curves are the 95% confidence limits of the fit.
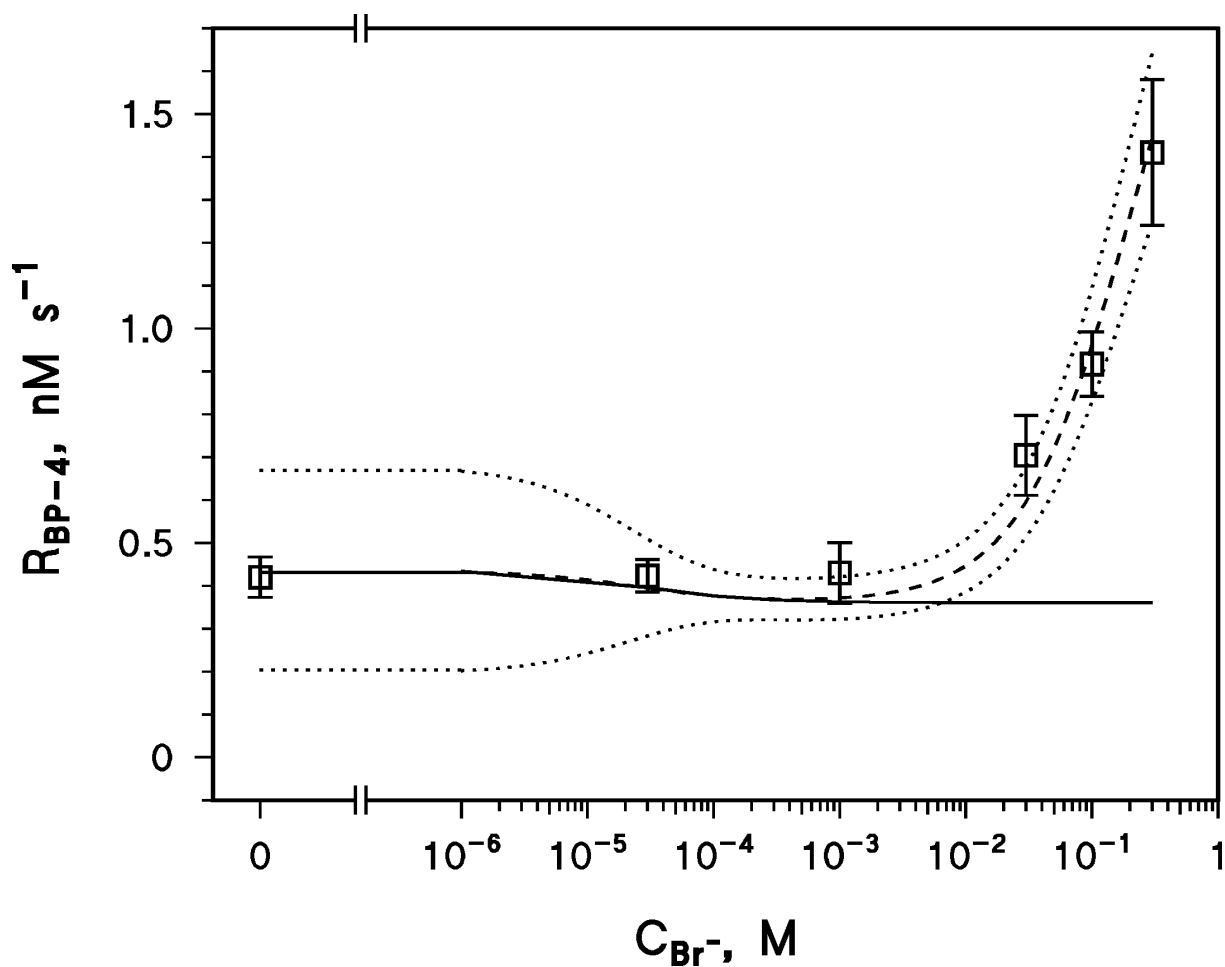
Figure 5. Initial BP-4 transformation rate (R_{BP-4}) as a function of bromide concentration, upon irradiation of 10 mM nitrate at pH 7.5. The dashed curve is the fit of experimental rate data with equation (17) (see the text for fixed and floating variables), the dotted ones are the 95% confidence limits of the fit. The solid curve represents the predicted trend of R_{BP-4} if reaction (11) is not operational.
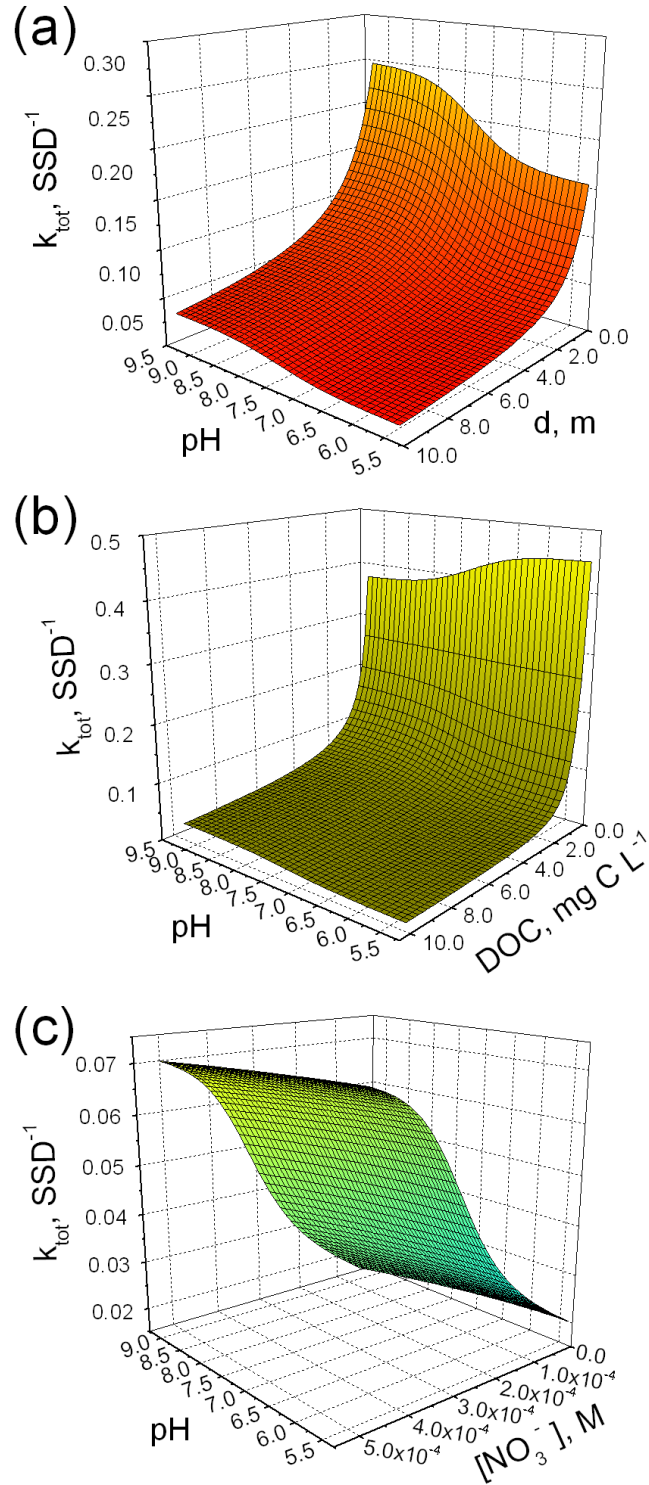
Figure 6. Modelled pseudo-first order transformation rate constant of BP-4, as a function of: **(a)** pH and depth; **(b)** pH and DOC; **(c)** pH and nitrate. When not set as variables, water chemistry parameters are as follows: 5 m depth, 3 mg C L^{-1} DOC, 0.1 mM nitrate, 1 μM nitrite, 1 mM inorganic carbon. Note that sunlight does not travel vertically in water and, therefore, 5 m depth means an actual light path of ~ 6 m (see SM).
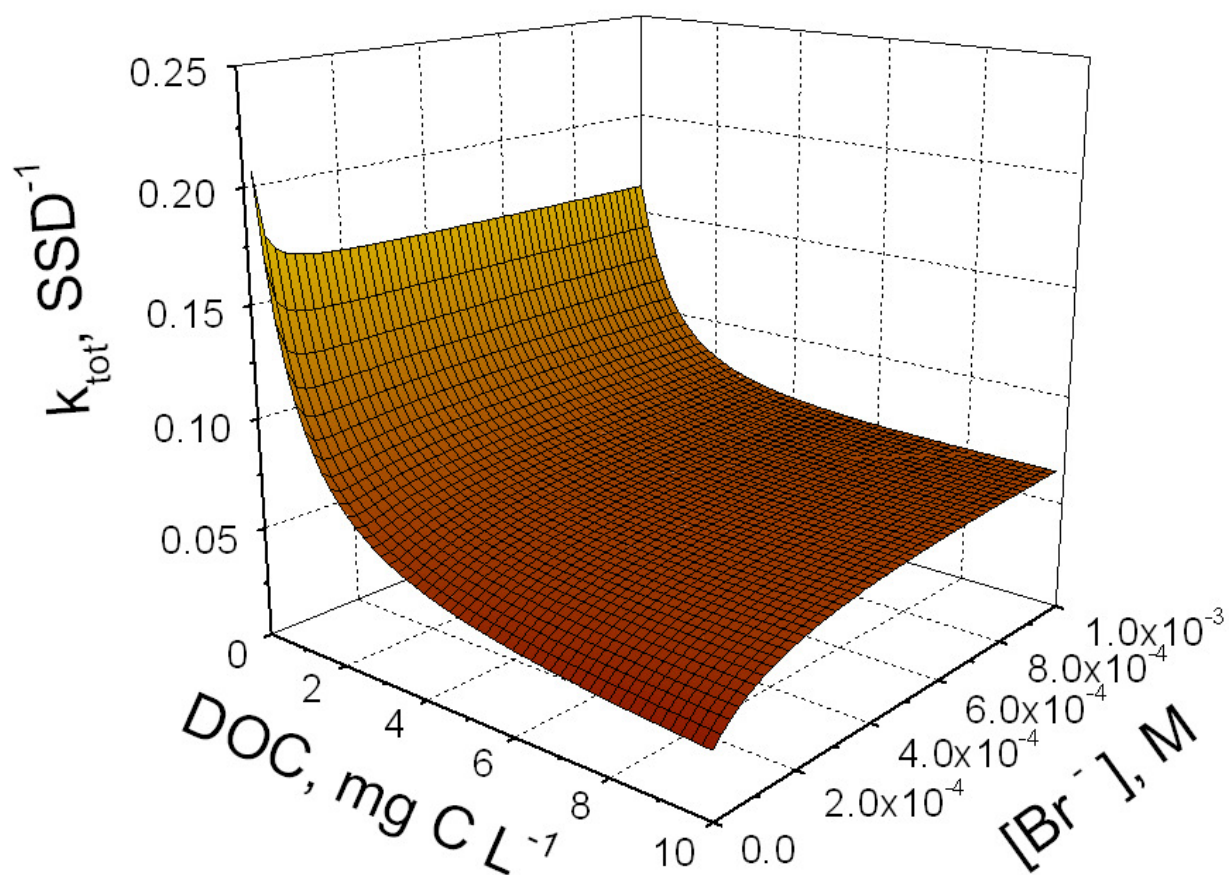
Figure 7. Modelled pseudo-first order transformation rate constant of BP-4, as a function of DOC and bromide. Other water parameters: 5 m depth, 0.1 mM nitrate, 1 μM nitrite, 1 mM inorganic carbon.
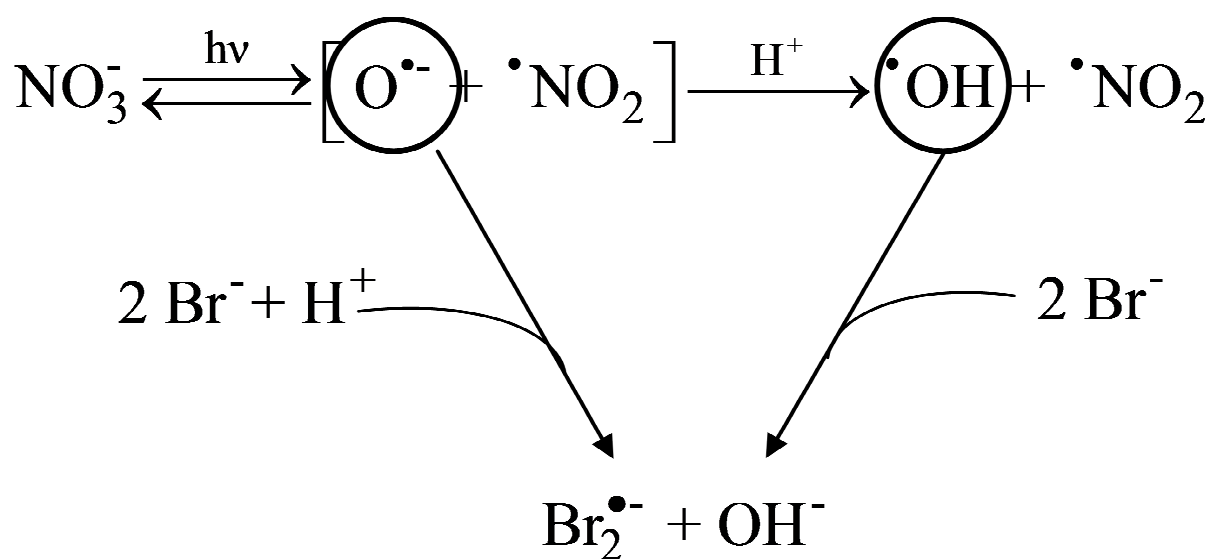
Scheme 1. Interaction between bromide and the fragments photogenerated by nitrate photolysis, in the solvent cage and in solution.